Driving With Hemianopia: IV. Head Scanning and Detection at Intersections in a Simulator

Alex R. Bowers, Egor Ananyev, Aaron J. Mandel, Robert B. Goldstein, and Eli Peli

Schepens Eye Research Institute, Massachusetts Eye and Ear, Department of Ophthalmology, Harvard Medical School, Boston, Massachusetts

Correspondence: Alex R. Bowers, Schepens Eye Research Institute, 20 Staniford Street, Boston MA 02114; alex_bowers@meei.harvard.edu.

Submitted: July 5, 2013
Accepted: January 10, 2014

Citation: Bowers AR, Ananyev E, Mandel AJ, Goldstein RB, Peli E. Driving with hemianopia: IV. Head scanning and detection at intersections in a simulator. *Invest Ophthalmol Vis Sci*. 2014;55:1540–1548. DOI:10.1167/iovs.13-12748

Purpose. Using a driving simulator, we examined the effects of homonymous hemianopia (HH) on head scanning behaviors at intersections and evaluated the role of inadequate head scanning in detection failures.

Methods. Fourteen people with complete HH and without cognitive decline or visual neglect and 12 normally sighted (NV) current drivers participated. They drove in an urban environment following predetermined routes, which included multiple intersections. Head scanning behaviors were quantified at T-intersections ($n = 32$) with a stop or yield sign. Participants also performed a pedestrian detection task. The relationship between head scanning and detection was examined at 10 intersections.

Results. For HH drivers, the first scan was more likely to be toward the blind than the seeing hemifield. They also made a greater proportion of head scans overall to the blind side than did the NV drivers to the corresponding side ($P = 0.003$). However, head scan magnitudes of HH drivers were smaller than those of the NV group ($P < 0.001$). Drivers with HH had impaired detection of blind-side pedestrians due either to not scanning in the direction of the pedestrian or to an insufficient scan magnitude (left HH detected only 46% and right HH 8% at the extreme left and right of the intersection, respectively).

Conclusions. Drivers with HH demonstrated compensatory head scan patterns, but not scan magnitudes. Inadequate scanning resulted in blind-side detection failures, which might place HH drivers at increased risk for collisions at intersections. Scanning training tailored to specific problem areas identified in this study might be beneficial.

Keywords: head movements, driving, rehabilitation, detection, hemianopia

In previous papers in this series, we addressed the effect of homonymous hemianopia (HH) on detection performance[1,2] and vehicle control[3] in a driving simulator. Individuals with HH may be able to compensate for their hemifield loss by scanning with eye and/or head movements into the blind field; here we address head scanning behaviors. Several studies have recorded eye and head movement behaviors of people with HH when performing laboratory-based tasks[4–9]; however, oculomotor behaviors observed during such highly constrained laboratory tasks do not necessarily generalize to everyday visually guided behaviors.[10,11] Currently, there is only limited information about scanning behaviors of people with HH in real-world tasks such as driving.[12–15] An important question is the extent to which they adopt scanning behaviors that effectively compensate for their hemifield loss.

Szylk et al.[12] reported that three participants with HH had greater head position variability than control drivers in a driving simulator, but did not evaluate whether there were any blind/seeing-side asymmetries in that variability. Furthermore, head position was quantified from videotape recordings frozen only once every 4 seconds; thus, many head movements may have gone undetected. In a more recent simulator study,[13] two participants with HH were found to make fewer head movements than controls.

Wood et al.[14] conducted an on-road study in which head movements were qualitatively analyzed from video footage. Scorers, masked to the HH side and road test outcome, reviewed the videos to determine the number of small and large head movements to the blind and seeing sides. Although there was a trend for drivers with HH ($n = 30$) to make more head movements than controls, the main finding of interest was that drivers rated as safe on the road test made significantly more head movements to the blind than the seeing side; there was no such difference between blind-side and seeing-side scanning for unsafe drivers. These data suggest that safe drivers were adopting compensatory head scanning. However, it is unknown whether these scanning patterns resulted in better detection of blind-side hazards.

A recent study[15] of eye and head scanning behaviors of people with HH in a virtual intersection collision avoidance task found that participants who performed well on the task (had few collisions) exhibited more active blind-side scanning behaviors, including larger blind-side scans and more frequent gaze shifts, than participants who performed less well (had more collisions). These findings suggest a direct relationship between scanning behaviors and detection of potential collisions. However, from 22.5 m before the intersection, participants were unable to slow down or stop (as would be the case when approaching an intersection in on-road driving), which might have affected the scanning behaviors.

In an on-road study of drivers with HH,[16] the majority of detection failures occurred at intersections, suggesting that

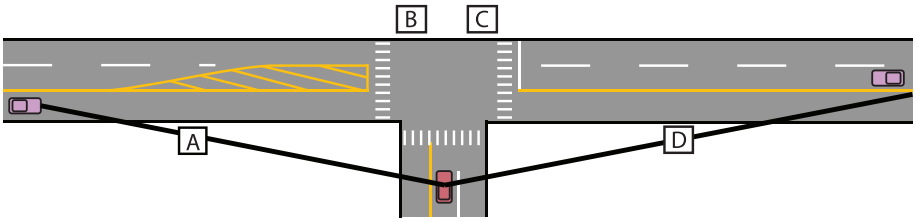

Figure 1. Schematic, approximately to scale, of the clear-sight triangle (*thick black lines*) for a stop-controlled intersection at a 30-mph cross street.[17] A driver with HH would have to execute a gaze scan of approximately 85° to view the whole area of the sight triangle on the blind side. Pedestrians were placed at locations A and D to evaluate whether drivers with HH scanned sufficiently far to the blind side (to the left for left HH and to the right for right HH). Pedestrians were placed at B and C to evaluate whether HH also affected detection in more central parts of an intersection critical to safe execution of a turn maneuver.

many of the participants did not scan effectively; however, head movements were observed, not recorded. Indeed, the wide field of view that needs to be scanned at T-intersections must present an especially challenging situation for drivers with HH. To view the whole area of the clear-sight triangle[17] on the affected side (Fig. 1), drivers with HH would have to make a gaze scan of approximately 85° as they have no peripheral vision on that side. A scan of this magnitude would require a head movement as well as an eye movement. By comparison, on the seeing side they would not necessarily need to gaze scan the full 85°, perhaps only 65°, because objects could be detected with the intact peripheral vision. Nevertheless, they would still need to make a head movement, as well as an eye movement, as typical eye saccades are rarely larger than 15°.[18] Therefore, we would expect that drivers with HH would either rotate the head further, or would make larger eye saccades or more eye saccades toward the blind than the seeing side in order to view the full width of the sight triangle on that side.

In this study we quantified head scanning patterns of drivers with HH in simulated driving scenarios and evaluated whether they adopted compensatory scanning strategies on approach to T-intersections with stop or yield signs. Specifically, we predicted that they would show the following compensatory behaviors for large head scans starting from the straight-ahead position: (1) a greater proportion of scans toward the blind side than for normally sighted drivers to the corresponding side; (2) larger head scans to the blind than the seeing side, and larger than those of normally sighted drivers; and (3) lower rates of not scanning to the blind side relative to those of normally sighted drivers to the corresponding side. Finally, we evaluated the relationship between head scanning and detection performance to determine which aspects of scanning, such as failing to scan or not scanning sufficiently far into the blind hemifield, caused blind-side detection failures.

Methods

Participants

Fourteen people with complete[19] HH participated, including the 12 reported in our first paper[1] and 2 additional participants recruited at a later date. One of the original 12 was subsequently excluded from data analyses as the head tracking data were so poor that scans could not be reliably distinguished from noise for any of the drives. Thus a total of 13 participants with HH (6 with right HH) were included in analyses. None had visual neglect (Bells test[20] and Schenkenberg Line Bisection tests[21]) or significant cognitive decline ($\geq$24 on Mini Mental State Examination[22]). All had HH of at least 4 months duration and visual acuity of 20/30 or better in each eye. Two with left HH had hemiparesis but were able to use the standard vehicle controls (gas and brake pedals, steering wheel, horn, and so on).

In addition, a group of 12 current drivers with no visual abnormalities (normal vision; NV) and an age and sex distribution similar to that of the HH group participated. The study was conducted in accordance with the tenets of the Declaration of Helsinki and approved by institutional review boards at both the Schepens Eye Research Institute and the Boston Veterans Administration Healthcare System. Voluntary, written informed consent was obtained from all participants after a full explanation of the study procedures.

Apparatus

Participants drove in a PP1000-x5 simulator (FAAC Corp., Ann Arbor, MI) with five 29-inch cathode ray tube (CRT) monitors (1024 $\times$ 768 resolution at 60 Hz) providing a 225° horizontal by 32° vertical field of view.[1,3,23] The wide field of view enabled realistic intersection scenarios to be presented. The simulator included all of the controls usually found in a car with automatic transmission. Software recorded usage of all vehicle controls, locations of the participant's vehicle, and all other scriptable entities in the virtual world at a 30-Hz sampling rate.

For head movement recording, a remote infrared (IR) system (TrackIR 3; NaturalPoint, Corvallis, OR) was used. Participants wore a lightweight head band with reflectors attached that enabled natural head movements. The IR source and tracking camera were mounted above the central screen of the simulator, approximately 1 m from the participant. The system tracked the head with 1° relative accuracy and a range of $\pm$70°, sufficient to capture large scanning movements at intersections. Head position data were collected at 60 Hz but were synchronized to the slower driving simulator data feed (30 Hz).

Procedures

In order to complete the full set of test drives, participants attended two driving simulator sessions, approximately 1 week apart. They wore habitual spectacle corrections. Each session started with acclimation to the simulator environment through a series of introductory drives that included all the elements of the test drives. Participants drove on the right side of the road and were instructed to drive in a manner that "resembled [their] actual driving behavior as much as possible," and "to obey all standard rules of the road." They were told that they should "move their head and eyes as they would normally when driving." They were not given any instructions or feedback about scanning at intersections.

After acclimation, participants completed a series of test drives at each session[1,3] including four routes on city roads (30 mph) with a variety of traffic situations and intersections. Prerecorded audio cues (e.g., "turn left at next intersection")

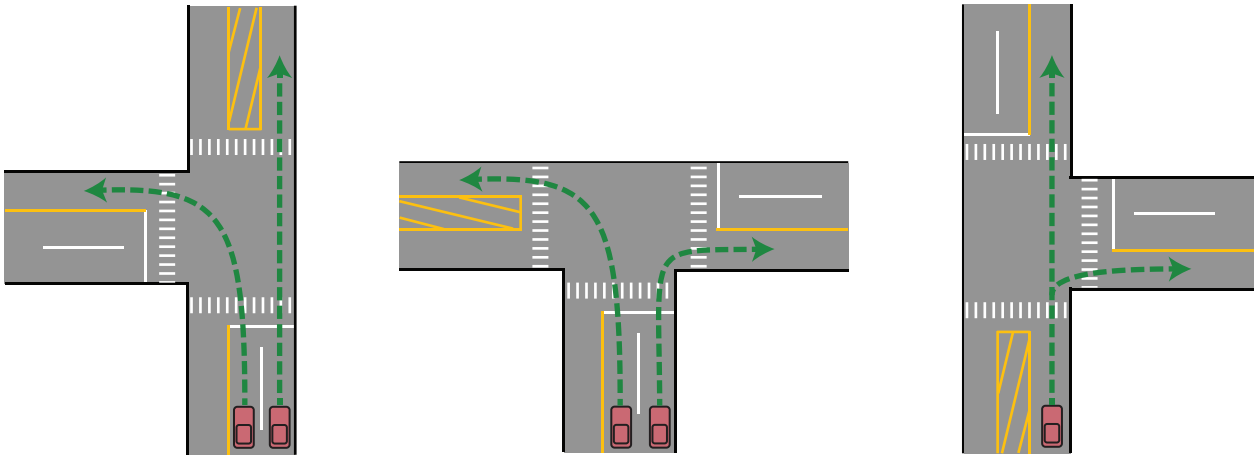

FIGURE 2. Head scanning was evaluated at T-intersections with either a stop or yield sign. The intersections had three configurations: no incoming road on the right (NIR, shown at *left*), incoming roads on both sides (IB, *center*), and no incoming road on the left (NIL, shown at *right*).

directed the driver along the routes, designed to be completed in 8 to 10 minutes. Participants performed a detection task while driving, pressing the horn button as soon as a pedestrian was seen.[1]

Head movements were recorded during each test drive. The head tracker was calibrated using a 5-point sequence (–67.5°, –22.5°, 0°, 22.5°, and 67.5°) at the start and end of every drive. The time to complete each simulator session (acclimation and test drives) ranged between 2 and 3 hours. The participants were encouraged to take breaks and step out of the simulator as needed between drives.

Intersections

Head movement behaviors were evaluated at T-intersections with either a stop or a yield sign, at which all drivers would have to scan before entering the intersection. Although there were other types of intersections in the virtual world (including Y, +, and rotaries), they did not occur with sufficient frequency to be included in analyses. The T-intersections had three configurations (Fig. 2): no incoming road on right (NIR; median 11 for the two sessions), incoming roads on both sides (IB; 12 for the two sessions), and no incoming road on left (NIL; 9 for the two sessions). To provide realistic scenarios and encourage head scanning, we programmed cross traffic on approximately one-third of intersections in each drive.

Analyzing Head Scanning at Intersections

Head movements on approach to intersections typically comprised a series of single large rotations taking the head away from the straight-ahead position to the left or right side with a subsequent single large rotation in the opposite direction bringing the head back to the center, sometimes directly continuing with a large rotation to the other side (see Supplementary Appendix A1). A head scan was defined as a lateral head rotation (yaw movement) that took the head away from the straight-ahead position for at least 0.2 seconds and that represented a net monotonic change in angle of more than a three-tier threshold (4°, 6°, and 10°), depending on the distance from the intersection (see Supplementary Appendix A1 for details). Head scans were analyzed from 100 m before the intersection to the point at which the front axle of the car crossed the white stop line on entering the intersection. The 100-m distance was selected for two reasons: It was approximately twice the minimum recommended[17] approach sight distance for an intersection with a yield sign; and, based on data from this study, it was also the distance at which head scan magnitudes first started to increase as drivers approached T-intersections in our driving simulator (Fig. 3).

An algorithm was developed to quantify the direction and magnitude of each head scan (see Supplementary Appendix A1). Scan direction was assigned a left/right binary code in terms of whether the scan took the head away from the straight-ahead position toward the left side or the right side. To analyze head scan magnitudes, the 100-m approach distance was split into three unequal pseudo-logarithmic bins: 30 to 100, 10 to 30, and 0 to 10 m. For each subject, a median scan magnitude was calculated for each bin. Only bins with two or more scans were considered.

In addition to analyzing when there were scans, we also analyzed situations when there were no scans: (a) not scanning in the direction with no incoming road and (b) not scanning in the direction of an incoming road. In the first situation, we did not expect NV participants to scan; however, we predicted that participants with HH would scan when there was no incoming road on their blind side, but not their seeing side. In the second situation, when there was an incoming road, both NV and HH participants should have scanned in that direction; therefore not scanning was classified as a failure to scan.

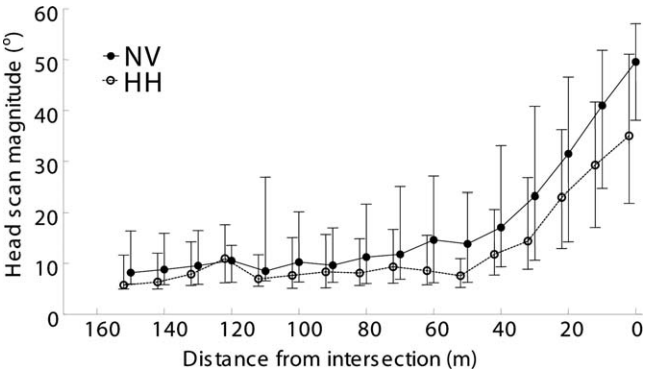

FIGURE 3. Median head scan magnitudes on approach to intersections for participants with NV and HH. As distance to the intersection decreased, scan magnitudes increased; this increase started at approximately 100 m before the intersection. Data were pooled in 10-m bins, with data in the 0-m bin from 0 to 9.99 m and so on. Each bin includes all scans for all participants (either HH or NV) within that range of distances from the intersection. *Error bars* represent the interquartile range.

Table. Participant Characteristics

	LHH, $n = 7$	RHH, $n = 6$	NV, $n = 12$
Current driver, *n* (%)	3 (43)	3 (50)	12 (100)
Male, *n* (%)	6 (86)	4 (67)	9 (75)
Age, y, mean (SD)	54 (9)	46 (15)	51 (13)
MMSE* score, mean (SD)	29 (0.7)	28 (1.3)	28 (1.8)
Hemianopia caused by stroke, *n* (%)	7 (100)	4 (67)	NA
Years since onset, median (IQR)	3.3 (1.7–5.7)	4.1 (1.8–6.1)	NA

* Mini Mental State Examination.

Pedestrian Detection and Scanning at Intersections

To evaluate detection at intersections, a stationary pedestrian figure (2 m tall, wearing a white top and blue trousers) appeared at 10 intersections across the two sessions: four times at location A (twice on a right turn and twice on a left turn) and twice at each of the other locations, B, C, and D (Fig. 1). None of the intersection pedestrians (I-Peds) presented an imminent threat, as they were stationary. Rather they were used to evaluate detection at locations where moving traffic could be a potential hazard for a turning vehicle. There was cross traffic on intersections with and without I-Peds; therefore, there was always a possibility that there could have been a moving car in the vicinity of an I-Ped.

Based on the American Association of State Highway and Transportation Officials[17] recommended sight distance for a stop-controlled intersection with a 30 mph cross street, I-Peds were placed 40 m along the sidewalk from the intersection at location A (to the left) and D (to the right) to evaluate whether drivers with left HH and right HH scanned sufficiently far (85°) to their blind sides, respectively. In addition, I-Peds were placed at locations B and C to evaluate whether HH affects detection in more central parts of an intersection critical to safe execution of a turn maneuver (addressed in detail in the first paper in this series[1]). Each I-Ped appeared as the driver was slowing to a stop at the intersection and disappeared as soon as the driver had completed a turn; only one I-Ped appeared at a time. There were a total of 154 pedestrian appearances across the two sessions in a variety of situations,[1] of which only 10 were at intersections.

At intersections with I-Peds, head scans in the direction of the I-Ped were analyzed between the time when the I-Ped appeared and either the time of the horn press or the time when the I-Ped disappeared, whichever occurred first (see Supplementary Figs. A2.1–A2.4 in Supplementary Appendix A2). Each I-Ped event was then categorized as (1) driver failed to scan in the direction of the I-Ped and did not detect; (2) driver scanned in the direction of the I-Ped but did not detect; or (3) driver scanned in the direction of the I-Ped and detected.

Statistical Analyses

Mixed-effects binary logistic regressions were conducted to evaluate the effect of vision status (NV, left HH [LHH], and right HH [RHH]) on whether a scan was to the left, whether there were no scans in a specific direction, and whether I-peds were detected. Participants were included as a random factor. In addition, as we expected that intersection configuration (NIR, IB, NIL; Fig. 1) would affect scanning patterns, we included this as a within-subjects factor for analyses of scan directions. The effect of maneuver (left turn, right turn, straight across) was not analyzed as there were insufficient numbers of intersections for both intersection configuration and maneuvers to be analyzed as separate factors. Results of the binary logistic regression analyses are plotted as the estimated mean proportions with 95% confidence limits; data in the text are reported in terms of the observed proportions.

A repeated-measures multivariate ANOVA was used to analyze the scan magnitude data with magnitude of right and left scans as the dependent variables, distance bin as the within-subjects variable, and vision status as the between-subjects variable. Bonferroni corrections were applied to all within-subject multiple comparisons (paired *t*-tests). Nonparametric analyses were also performed, with results comparable to the parametric analyses. R (Version 2.15.2[24]) statistical package was used in data analyses. For mixed-effects logistic regressions, the *glmer* function of R package *lme4*[25] was used. An alpha level ≤ 0.05 was taken to indicate statistical significance

Results

Sample Characteristics

The HH group included six current drivers (driving at least on a limited basis), four who had stopped driving within the past year, and three who had stopped driving within the past 3 to 11 years. Stroke was the main cause of the HH, with the time since onset of the HH ranging from 4 months to 28 years (Table). As planned, the HH and NV groups were not significantly different in terms of age, sex, and Mini Mental State Examination scores (all $P > 0.5$). All participants had started driving at age 19 or younger; the only exceptions were one with HH and one with NV, who had started driving at the ages of 23 and 27 years, respectively.

Scan Patterns

Although there were no significant differences among the vision groups in the total number of scans ($F_{(2,22)} = 1.465$, $P = 0.253$), there were notable between-group differences in the proportions of leftward scans ($\chi^2_{(2)} = 11.465$, $P = 0.003$; Fig. 4). Overall on approach to an intersection, the LHH group had a significantly higher proportion of leftward scans (76%) than the NV and RHH groups (59% and 48%, respectively; data pooled across the three intersection configurations). By comparison, there was a trend for the RHH group to have a lower proportion of leftward scans (i.e., a higher proportion of rightward scans) than the NV group. As expected, the proportion of leftward scans was highest when there was an incoming road on the left only (74%) and lowest when there was no incoming road on that side (41%, data pooled across all participants; $\chi^2_{(2)} = 96.906$, $P < 0.001$). However, there was a significant interaction between this pattern and the side of the HH ($\chi^2_{(4)} = 46.321$, $P < 0.001$). Specifically, pairwise comparisons revealed that the RHH group made a significantly lower proportion of leftward head scans (i.e., a higher proportion of rightward scans) than the NV and LHH drivers ($P = 0.008$ and $P < 0.001$, respectively) when there was no incoming road on their blind right side (NIR; Fig. 4), while the LHH group made a significantly higher proportion of head scans to their blind left side than the NV and RHH drivers (both P values < 0.001) when there was no incoming road on that side (NIL; Fig. 4). In fact, for both HH groups, the proportion of blind-side scans was similar irrespective of whether or not there was an incoming road on that side.

Considering the scan patterns in more detail, Figure 5 summarizes the directions of the first two scans for each intersection configuration. Across all configurations, there is a clear trend for the LHH group to have leftward-dominated scan

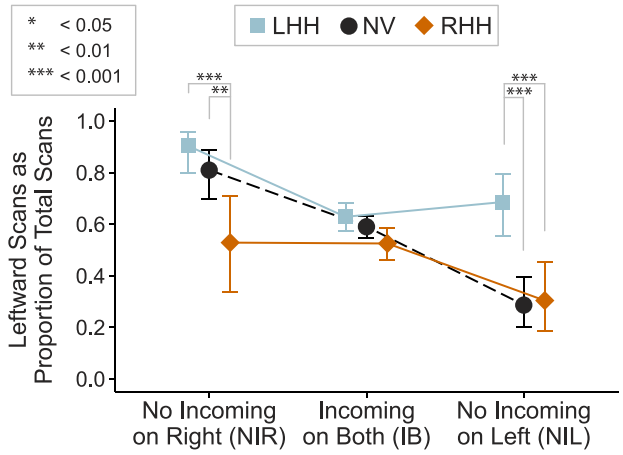

FIGURE 4. Mean proportion of leftward scans for each intersection configuration and each vision group. Overall, drivers with LHH had the highest proportion of leftward scans (to their blind side) while drivers with RHH had the lowest proportion of leftward scans, that is, a higher proportion of scans to their blind right side. For the NV group, the proportion of leftward scans was modified when there was no incoming road on either the right or left (NIR and NIL, respectively). However, for the HH groups, the proportion of leftward scans changed only when there was no incoming road on their seeing side, but not on their blind side. *Error bars* are 95% confidence intervals.

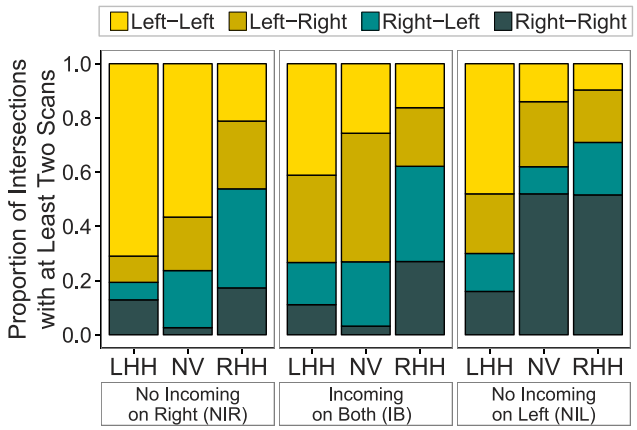

FIGURE 5. Directions of the first two scans for each intersection configuration. The LHH group had leftward-dominated scan patterns (Left-Left and Left-Right) while the RHH group had rightward-dominated scan patterns (Right-Right and Right-Left).

patterns (Left-Left and Left-Right) and the RHH group to have rightward-dominated scan patterns (Right-Right and Right-Left).

Scan Magnitudes

For all groups, the magnitude of the leftward and rightward scans increased as distance to the intersection decreased ($F_{(2,44)} = 21.277$, $P < 0.001$; Fig. 6). Overall, the head scan magnitudes for the two HH groups were smaller than those of the NV group ($F_{(2,22)} = 5.792$, $P < 0.001$; Figs. 3, 6). This pattern was especially evident for the right scans closer to the intersection. Contrary to our expectations, for the HH groups, blind-side scans were not larger than seeing-side scans. For the LHH and NV groups there were no significant differences in the overall magnitudes of right and left scans (LHH: $t_{(6)} = 0.618$, $P = 1$; NV: $t_{(11)} = 0.481$, $P = 1$). However, for the RHH group, right (blind side) scans were smaller than left (seeing side) scans ($t_{(6)} = 5.900$, $P = 0.004$), especially in the 0- to 10-m bin (compare Fig. 6, left and right).

Not Scanning

As expected, when there was no incoming road on one side, the NV participants were unlikely to scan in that direction; they did not scan to the right at approximately 73% of intersections with no incoming road on the right (NIR) and did not scan to the left at approximately 71% of intersections with no incoming road on the left (NIL; Fig. 7). Homonymous hemianopia participants demonstrated similar behaviors only when there was no incoming road on their seeing side. Therefore, compared to the RHH group, the LHH and NV groups were more likely to not scan to the right when there was no incoming road on the right side (NIR; $P = 0.001$ and $P = 0.002$, respectively); and compared to the LHH group, the RHH and NV groups were significantly more likely to not scan to the left on intersections with no incoming road on the left side (NIL; both P values < 0.001).

In addition, we evaluated failures to scan in the direction of an incoming road. For failures to scan to the left when there was a road on the left, we combined data for incoming roads on both sides (IB) and no incoming road on the right (NIR; i.e., an incoming road on the left only). Similarly, for failures to scan to the right when there was a road on the right, the IB and NIL configurations were combined. Overall, failure rates were significantly higher for rightward than for leftward scans ($\chi^2_{(1)} = 51.930$, $P < 0.001$; Fig. 8). Contrary to our prediction, drivers with HH did not have lower blind-side scan failure rates than did the NV drivers to the corresponding side. Specifically, right scan failure rates were not significantly different for the RHH and NV groups, and left scan failure rates were not significantly different for the LHH and NV groups ($P = 0.935$ and $P = 0.806$, respectively; Fig. 8).

Detection Rates and Scanning Behaviors at Intersections

The LHH group had significantly lower detection rates than the NV group for the pedestrian at the far left of the intersection (I-Ped A), while the RHH group had significantly lower detection rates than the NV group for pedestrians at center right (I-Ped C) and far right (I-Ped D) (Fig. 9). As expected, all three groups had high detection rates for the pedestrian at center left (I-Ped B) that appeared on a left turn, and was likely in view for most of the turn maneuver.

Scanning behaviors were analyzed to determine the causes of detection failures (Supplementary Appendix A2). For I-Ped A, not scanning to the left accounted for a similar proportion of detection failures in the three vision groups (Fig. 10); in all cases when there was a failure to scan, I-Ped A was not detected. In addition, for the HH groups (but not the NV group), there were detection failures even when leftward head scans were made (Fig. 10). The rate of scanning and failing to detect I-Ped A was higher for the LHH than the NV group ($P = 0.007$). When I-Ped A was detected, the magnitude of the leftward head scan was similar (medians 49°–55°) for the three groups. For the LHH group, detection in this case would also have required eye scanning, as a 55° head scan would not suffice. When detection did not occur, the leftward head scans of RHH drivers were smaller (median 32°, interquartile range [IQR] 17°–33°) than when detection did occur (median 49°, IQR 47°–61°). However, the difference in scan magnitudes between detection not occurring and occurring was less

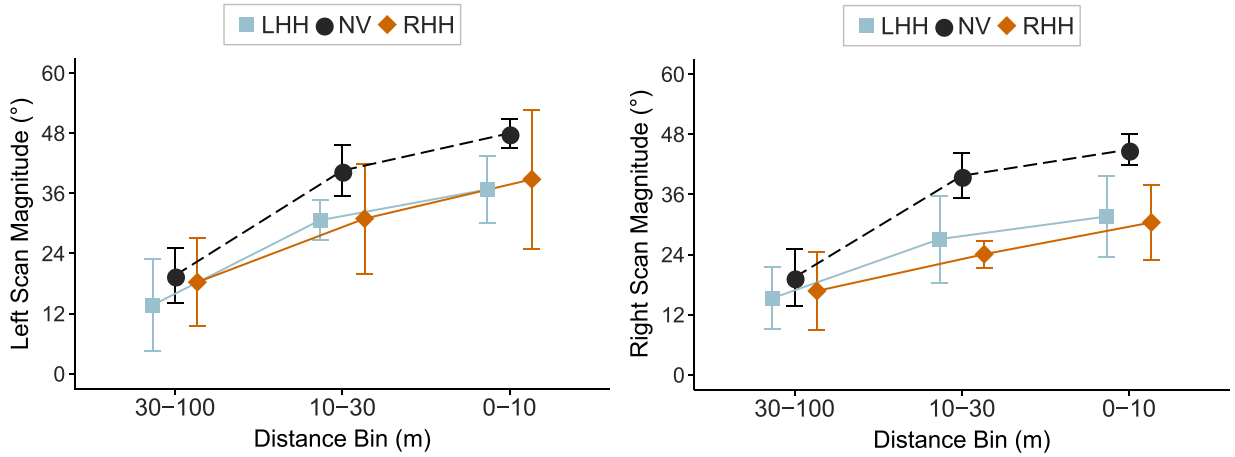

Figure 6. Mean magnitude of scans on approach to intersections: scans to the left and scans to the right. For all vision groups, scan magnitude increased as distance to the intersection decreased. Scan magnitudes of drivers with HH tended to be smaller than those of NV drivers. *Error bars* are 95% confidence intervals.

marked for the LHH drivers (medians 42°, IQR 27°–56° and 55°, IQR 53°–62°, respectively).

For I-Ped C, not scanning to the right was the main reason for detection failures by RHH participants (Fig. 10). In the majority of cases, I-Ped C was detected only when the head was turned at least slightly to the right of the straight-ahead position after the pedestrian appeared. Similarly, for I-Ped D, not scanning to the right was also a major reason for detection failures by RHH participants. In addition, however, there were detection failures even when rightward scans were made. The median magnitude of these scans was 41° (IQR 40°–46°), similar to that of the leftward head scan for the situations in which the LHH group scanned but failed to detect I-Ped A.

Discussion

Consistent with our hypothesis, when approaching an intersection, the HH groups showed head scanning behaviors that tended to be dominated by large scans from the straight-ahead position that were directed toward their blind side. They scanned more frequently into their blind hemifield than did the NV group to the corresponding side, and the first scan was more likely to be toward the blind than the seeing hemifield. These blind side–dominated scan patterns are consistent with prior studies of patients with HH[14,15,26] and provide evidence of compensatory behaviors in response to the hemifield loss. However, contrary to our expectations, there was no evidence of compensation in scan magnitudes; blind-side head scans were not larger than seeing-side head scans. In fact, for the RHH group, head scans to the blind right side were smaller than scans to the seeing left side. Smaller scans to the blind than the seeing side are consistent with gaze behaviors observed by Papageorgiou et al.[15] in their simulated intersection collision avoidance task. It is curious that HH drivers, despite being aware of their vision loss (as evidenced by increased scanning to the blind side), do not also compensate by head scanning farther into the blind than the seeing side at intersections. This behavior is consistent with the lack of increased scanning magnitude (relative to NV observers) demonstrated by people with severe peripheral visual field restrictions (due to retinitis pigmentosa) when walking[27,28] and may occur because they do not know how far to scan, as there is no guidance from peripheral vision.

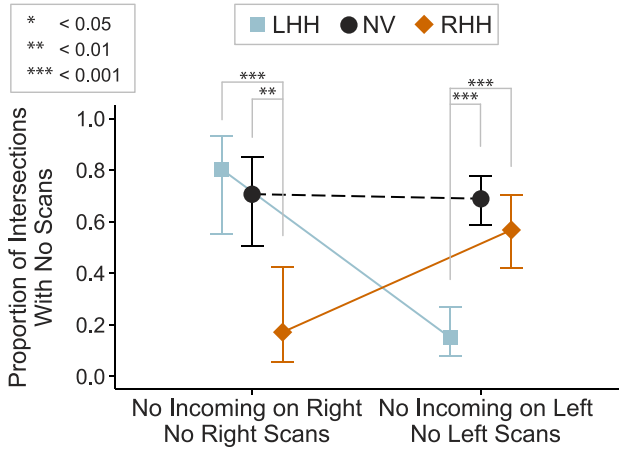

Figure 7. Mean proportion of intersections at which participants did not scan when there was no incoming road on one side. Drivers with RHH had low rates of not scanning to the blind right side when there was no incoming road on the right (NIR). Drivers with LHH had low rates of not scanning to the blind left side when there was no incoming road on the left (NIL). (There were medians of 9 NIL and 11 NIR intersections per participant.) *Error bars* are 95% confidence intervals.

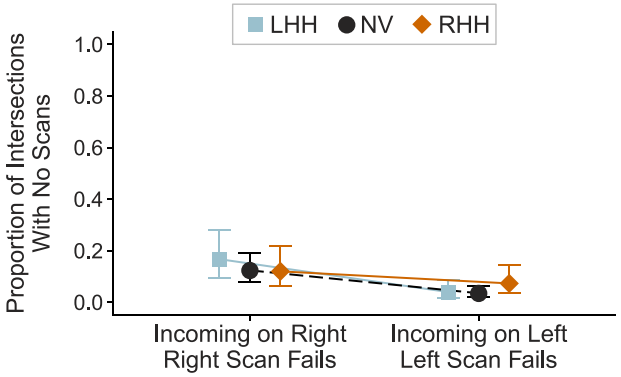

Figure 8. Mean proportion of intersections at which participants failed to scan when there was an incoming road on one side. For the HH groups, rates of failing to scan to the blind side were similar to those of the NV group to the corresponding side. *Error bars* are 95% confidence intervals.

Investigative Ophthalmology & Visual Science

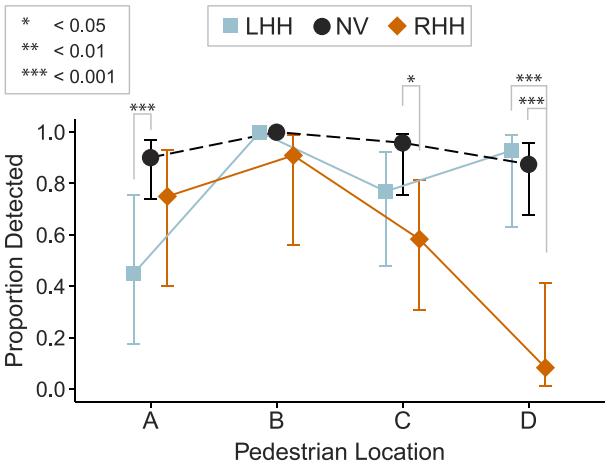

Figure 9. Mean detection rates for each of the intersection pedestrians (I-Peds) for the three vision groups. With the exception of I-Ped B, the HH groups had significantly lower detection rates than the NV group for I-Peds on their blind side. A, B, C, and D refer to the pedestrian locations at far left, center left, center right, and far right, respectively (see Fig. 1). *Error bars* are 95% confidence intervals.

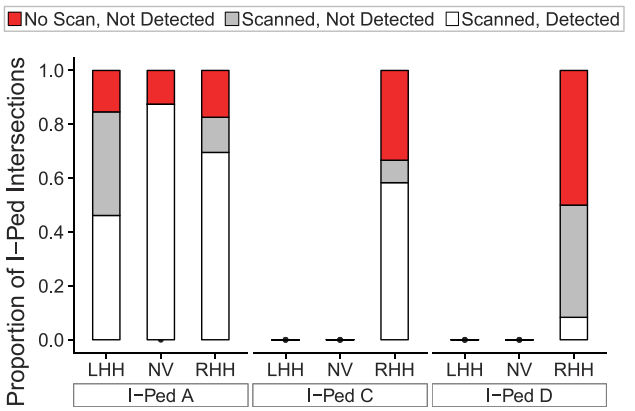

Figure 10. Reasons for I-Ped detection failures in each vision group for situations in which scanning was necessary to see the I-Ped. Inadequate scan magnitude (*gray shading*) was the main reason LHH drivers failed to detect I-Ped A on their blind left side. By comparison, in the RHH group, failing to scan (*red shading*) to the right and inadequate scan magnitudes (*gray shading*) contributed approximately equally to detection failures for I-Ped D on their blind right side. LHH and NV participants could see I-Peds C and D without scanning; hence, no data are reported. Data are pooled across participants in each group. A, C, and D refer to the pedestrian locations at far left, center right and far right, respectively (see Fig. 1).

When approaching a T-intersection with incoming roads on both sides, the NV group typically scanned to the left first, followed by a scan to the right. The scan pattern of the LHH group also started with a scan to left, but was more commonly followed by another scan to the left than by a scan to the right. By comparison, the typical scan pattern of the RHH group started with a scan to the right, followed by either another scan to the right or a scan to the left. When there was no incoming road on one side, NV drivers modified their scanning behaviors by scanning less often in that direction. When there was no incoming road on the seeing side, HH drivers also modified their scan patterns in a similar manner. However, when there was no incoming road on the blind side, their scan patterns did not change, as there was no information from peripheral vision to indicate whether or not a scan was needed in that direction.

We also examined the extent to which HH participants failed to scan to an incoming road on their blind side. Surprisingly, their failure rates were similar to those of the NV group in the corresponding directions (Fig. 8). However, unlike drivers with NV, drivers with HH do not have any information from their peripheral vision on the blind side; therefore, we might have expected lower failure-to-scan rates to an incoming road on the blind side. The similarity of the responses to those of the NV drivers suggests that the behavior was well established from the time that vision was intact and was not modified by the lack of visual stimuli; that is, these findings suggest a lack of effective compensation for the hemifield loss.

Left HH drivers detected only 46% of I-Peds at location A on the far left of the intersection, while the RHH drivers detected only 58% and 8% of I-Peds at locations C and D, on the near and far right, respectively. These results are consistent with data from an on-road study in which the majority of interventions for drivers with HH occurred as a result of failures to detect other vehicles and pedestrians at intersections.[16] For I-Ped A, the rates of failing to detect due to a lack of a leftward head scan after the I-Ped appeared were similar for the NV and HH groups, and this was the only reason for failing to detect in the NV group. However, for the HH groups, detection failures were also a result of insufficient scan magnitudes. This is not surprising for the LHH group, as they would have had to scan farther into the blind field (85°) than the RHH and NV groups to detect I-Ped A. Interestingly, when I-Ped A was detected, there were no differences in the median head scan magnitudes among the NV and HH groups (medians 49°–55°), yet a larger-magnitude head scan might have been expected for the LHH group. Thus, in order to detect I-Ped A, LHH drivers must have executed a large leftward eye movement, of at least 30°, in addition to the 55° leftward head scan. This is a much larger eye movement than is typically made during walking (usually less than 15°).[18] I-Ped A was detected by the LHH group only on approximately one-third of occasions when there was a leftward head scan (Fig. 10), suggesting that the accompanying eye scan was often insufficiently large. When I-Ped A was not detected, the range of head scan magnitudes of the LHH group was very wide and overlapped with the range of magnitudes when detection occurred, suggesting that the detection failures were due to insufficient eye movement magnitudes in these instances. By comparison, for the RHH group, the magnitudes of the left head scans were noticeably smaller when I-Ped A was not detected (only approximately 30° rather than 49°–55°).

While the LHH and NV groups could detect I-Peds C and D (appearing on the near and far right of the intersection, respectively) using their peripheral vision, it was necessary for the RHH group to scan to the right. To detect I-Ped C before entering the intersection, even a small rightward scan from the straight-ahead position would be sufficient. However, in approximately 33% of cases, the RHH drivers failed to scan to the right and detect I-Ped C. This is concerning, as the inability to detect an incoming car from the near right while making a left turn may result in a collision. For I-Ped D, the high rate of detection failures in the RHH group was a result of both failing to scan to the right and insufficiently large rightward scans. However, the I-Ped D position does not represent an imminent threat for the driver during the turn maneuver, and the driver may expect to detect obstacles or dangers in this location after completing the turn. Nevertheless, drivers with RHH do need to be aware of potential hazards in the travel path to their right, such as pedestrians crossing the road as they exit the intersection at the end of a right turn maneuver.

There are two study limitations that need to be considered. First, the stationary pedestrians did not present an imminent

Investigative Ophthalmology & Visual Science

threat or hazard; therefore, detection deficits might have been overestimated. Second, the lack of an eye tracker in the simulator limited our ability to determine whether gaze fell on each I-Ped, whether (in the absence of larger head scans to the blind side) HH participants compensated with larger eye saccades, and whether an eye saccade might have been made to the blind side in some instances when a head scan was not made. Nevertheless, it is reasonable to assume that if an I-Ped on the blind side was not detected, gaze (head combined with eye movement) did not fall on the pedestrian and that the overall gaze scan was inadequate.

Three findings from our study have implications for rehabilitation of drivers with HH. First, in the absence of peripheral cues from their blind side, drivers with HH seem unaware of how far they need to scan into their blind hemifield. Even when they scanned into their blind field at intersections, the magnitude of their scans often fell short of that necessary to cover the complete area of the clear-sight triangle[17] or to detect an I-Ped at the extreme location in their blind hemifield. This may put drivers with HH at increased risk for collision incidents at intersections. Second, both LHH and RHH drivers failed to scan to their blind side at an alarmingly high proportion of intersections, which resulted in failures to detect I-Peds. This was particularly noticeable for the RHH group, who had higher rates of failing to scan to the blind side than did the LHH group. This is perhaps due to the RHH drivers perceiving less danger from traffic on the right. However, in the absence of the peripheral cues from the blind hemifield, it is especially important for the RHH drivers to scan to the right to identify potential hazards from that direction. Third, there was evidence in the data that insufficient attention was being allocated to the seeing side. Several drivers with LHH had high rates of failing to scan to the seeing side when there was a road on that side (in one case, 63%). Similarly, some RHH drivers failed to scan sufficiently far to the left at some intersections (as evidenced by the failures to detect I-Ped A, despite scanning in that direction). Furthermore, seeing-side scan magnitudes of the HH drivers were smaller than those of the NV drivers. This may be a result of a reluctance to scan too far into the seeing side, because the farther a person with HH scans toward the seeing side, the greater the area of the intersection that is no longer visible.

The general perception that traffic from the right poses fewer safety concerns than traffic from the left was evident in the data from the NV group as well as in prior on-road studies of NV drivers.[14,29] For the HH drivers, there appeared to be an interesting interplay between this perception and blind-side scanning behaviors. Drivers with LHH appeared to focus on scanning to the left at the expense of scanning to the right, while drivers with RHH seemed to underestimate the potential consequences of traffic hazards on the right as evidenced by the high rates of failing to scan to the blind right side. Training for drivers with HH should focus on addressing specific deficits in their scanning patterns. As well as establishing a consistent scanning pattern that includes looking to both sides, cues as to how far to turn the head and eyes (such as specific instructions to look into the blind hemifield until the sidewalk on the near side of the cross street is seen) may be helpful. In addition, drivers with RHH need to be educated about the potential of hazards on the right and should be encouraged to make secondary scans to the right[30] once they have entered the intersection.

In conclusion, this study provides a detailed quantification of head scanning behaviors of drivers with HH at intersections. Our results show patterns of compensatory behavior that occurred with respect to the frequency and direction, but not the magnitudes of the head scans. We also found a clear relationship between inadequate scanning (failing to scan or not scanning far enough) and failure to detect pedestrians at intersections. The rate of failing to head scan to an incoming road on the blind side was no less than that of the NV drivers for the corresponding side. Taken together with the results of prior studies,[1,2,11,15,31] the findings of the present study suggest that scanning patterns employed by some HH drivers may be insufficient for safe driving and that they might benefit from training tailored to the specific problem areas identified here.

Acknowledgments

Supported by National Institutes of Health Grants EY12890 (EP) and EY018680 (ARB). Driving simulator facilities were provided by Joseph Rizzo of the Center for Innovative Visual Rehabilitation at the Boston Veterans Administration Healthcare System.

Disclosure: **A.R. Bowers**, None; **E. Ananyev**, None; **A.J. Mandel**, None; **R.B. Goldstein**, None; **E. Peli**, None

References

1. Bowers AR, Mandel AJ, Goldstein RB, Peli E. Driving with hemianopia: I. Detection performance in a simulator. *Invest Ophthalmol Vis Sci*. 2009;50:5137–5147.
2. Alberti CF, Peli E, Bowers AR. Driving with hemianopia: III. Detection of stationary and approaching pedestrians in a simulator. *Invest Ophthalmol Vis Sci*. 2013;55:368–374.
3. Bowers AR, Mandel AJ, Goldstein RB, Peli E. Driving with hemianopia: II. Steering and lane position in a simulator. *Invest Ophthalmol Vis Sci*. 2010;51:6605–6613.
4. Ishiai S, Furukawa T, Tsukagoshi H. Eye-fixation patterns in homonymous hemianopia and unilateral spatial neglect. *Neuropsychologia*. 1987;25:675–679.
5. Hardiess G, Papageorgiou E, Schiefer U, Mallot HA. Functional compensation of visual field deficits in hemianopic patients under the influence of different task demands. *Vision Res*. 2010;50:1158–1172.
6. Pambakian AL, Wooding DS, Patel N, Morland AB, Kennard C, Mannan SK. Scanning the visual world: a study of patients with homonymous hemianopia. *J Neurol Neurosurg Psychiatry*. 2000;69:751–759.
7. Zihl J. Eye movement patterns in hemianopic dyslexia. *Brain*. 1995;118:891–912.
8. Mannan SK, Pambakian ALM, Kennard C. Compensatory strategies following visual search training in patients with homonymous hemianopia: an eye movement study. *J Neurol*. 2010;257:1812–1821.
9. Roth T, Sokolov AN, Messias A, Roth P, Weller M, Trauzettel-Klosinski S. Comparing explorative saccade and flicker training in hemianopia: a randomized controlled study. *Neurology*. 2009;72:324–331.
10. Martin T, Riley ME, Kelly KN, Hayhoe M, Huxlin KR. Visually-guided behavior of homonymous hemianopes in a naturalistic task. *Vision Res*. 2007;47:3434–3446.
11. Iorizzo DB, Riley ME, Hayhoe M, Huxlin KR. Differential impact of partial cortical blindness on gaze strategies when sitting and walking - an immersive virtual reality study. *Vision Res*. 2011;51:1173–1184.
12. Szlyk JP, Brigell M, Seiple W. Effects of age and hemianopic visual field loss on driving. *Optom Vis Sci*. 1993;70:1031–1037.
13. Hamel J, Kraft A, Ohl S, De Beukelaer S, Audebert HJ, Brandt SA. Driving simulation in the clinic: testing visual exploratory behavior in daily life activities in patients with visual field defects. *J Vis Exp*. 2012;67:e4427.
14. Wood JM, McGwin G, Elgin J, et al. Hemianopic and quadrantanopic field loss, eye and head movements, and driving. *Invest Ophthalmol Vis Sci*. 2011;52:1220–1225.

15. Papageorgiou E, Hardiess G, Mallot HA, Schiefer U. Gaze patterns predicting successful collision avoidance in patients with homonymous visual field defects. *Vision Res*. 2012;65: 25–37.
16. Bowers AR, Tant M, Peli E. A pilot evaluation of on-road detection performance by drivers with hemianopia using oblique peripheral prisms. *Stroke Res Treat*. 2012;2012: 176806.
17. American Association of State Highway and Transportation Officials. *A Policy on Geometric Design of Highways and Streets*. Washington, DC: AASHTO; 2004:657.
18. Bahill AT, Adler D, Stark L. Most naturally occurring human saccades have magnitudes of 15 degrees or less. *Invest Ophthalmol*. 1975;14:468–469.
19. Giorgi RG, Woods RL, Peli E. Clinical and laboratory evaluation of peripheral prism glasses for hemianopia. *Optom Vis Sci*. 2009;86:492–502.
20. Vanier M, Gauthier L, Lambert J, et al. Evaluation of left visuospatial neglect: norms and discrimination power of two tests. *Neuropsychology*. 1990;4:87–96.
21. Schenkenberg T, Bradford DC, Ajax ET. Line bisection and unilateral visual neglect in patients with neurologic impairment. *Neurology*. 1980;30:509–517.
22. Folstein MF, Folstein SE, McHugh PR. "Mini-mental state." A practical method for grading the cognitive state of patients for the clinician. *J Psychiatr Res*. 1975;12:189–198.
23. Peli E, Bowers AR, Mandel AJ, Higgins KE, Goldstein RB, Bobrow L. Design of driving simulator performance evaluations for driving with vision impairments and visual aids. *Transp Res Rec*. 2005;1937:128–135.
24. R Core Team. *R: A Language and Environment for Statistical Computing*. Vienna, Austria: R Foundation for Statistical Computing; 2012. Available at: http://www.R-project.org/.
25. Bates D, Maechler M, Bolker B, Walker S. lme4: linear mixed-effects models using Eigen and S4. R package version 1.0-5. 2013. Available at: http://CRAN.R-project.org/package=lme4.
26. Lovsund P, Hedin A, Tornros J. Effects on driving performance of visual field defects: a driving simulator study. *Accid Anal Prev*. 1991;23:331–342.
27. Vargas-Martin F, Peli E. Eye movements of patients with tunnel vision while walking. *Invest Ophthalmol Vis Sci*. 2006;47: 5295–5302.
28. Luo G, Vargas-Martin F, Peli E. The role of peripheral vision in saccade planning: learning from people with tunnel vision. *J Vis*. 2008;8(14):25.
29. Bao S, Boyle LN. Age-related differences in visual scanning at median-divided highway intersections in rural areas. *Accid Anal Prev*. 2009;41:146–152.
30. Romoser MRE, Fisher DL. The effect of active versus passive training strategies on improving older drivers' scanning in intersections. *Hum Factors*. 2009;51:652–668.
31. Bronstad PM, Bowers AR, Albu A, Goldstein RB, Peli E. Hazard detection by drivers with paracentral homonymous field loss: a small case series. *J Clin Exp Ophthalmol*. 2011;S5:001.

Investigative Ophthalmology & Visual Science

SUPPLEMENTARY ONLINE MATERIALS

APPENDIX 1: Head Movement Data Preprocessing and Head Scan Algorithm

Linear equations were fit to the head tracker calibrations that were performed at the start and end of each drive.[1] Each pair of pre- and post-drive calibrations were compared, and if the value of the calibration equations at 0° disagreed by more than 4° (suggesting that the headband moved during the drive), the head tracking data for that drive were discarded. This happened in less than 1% of drives.

Occasionally, frames were lost or optical characteristics of the system caused invalid 'spikes' of head position. Therefore, the collected head position data were processed with a median filter with a window of 0.5 s (15 frames). Also, head tracker data were prone to dropouts due to loss of signal for large head turns; such dropouts were automatically detected (as discontinuities in the time stamps) and removed from analysis (5% of all data collected). Periods of data dropouts were also marked on head movement plots that were used for manual inspection of the data.

One of our primary measures was a count of discrete head scans: We first determined discrete head movements and then determined which of those movements could be categorized as scans. Since, head rotations are similar to steering wheel rotations, we modified the algorithm of Reed and Green[2] to detect discrete head movements. They defined a discrete (steering wheel) rotation as a series of first-order angle differences that do not change sign for more than a set fraction of a second (0.33 s) and that represent a net monotonic change in angle of more than a given threshold in degrees (1°). We modified the method to (a) select thresholds appropriate for head rotations rather than steering wheel rotations and (b) used a three-tier angle magnitude threshold based on distance from the intersection. The time and magnitude thresholds were determined empirically by adjusting them so that the computationally determined counts of discrete head movements matched counts that were made manually by review of the filtered head movement signal. The time threshold (T_t) was 0.2 s. The three-tier magnitude threshold

($T_{m1\text{-}m3}$) was based on the minimum size of movement that we could reasonably expect with decreasing distance (d) to the intersection. The thresholds were derived from a computation of the minimum movement required to turn the head to the middle of the oncoming traffic lane on the right when there were two lanes in each direction in the cross street, a minimum movement of: 4° for 50m < d <=100m, 6° for 25m < d <=50m, and 10° for 0m <d<=25m. We also set an upper exclusion limit of 135°.

The algorithm was implemented by processing the first and second derivatives (equivalent to the velocity and acceleration of the head) of the smoothed head movement signal. Specifically, the first derivative represented "first order head angle differences." To take the second derivative, the first derivative of the head movement signal was further smoothed by a zero-delay forward-and-backward filter.[3] Using the second derivative, we determined the places where the first derivative changed sign, thus representing a change in direction of motion. The difference between the upper and lower bounds of the time stamps of these direction changes gave the spans of time where the head was moving in a single direction. If the time span exceeded the threshold T_t, and the magnitude of the change exceeded T_m, then we counted it as a discrete head movement.

Once discrete head movements were identified, we then determined which part of the head movement constituted a head "scan". A head scan was defined as that portion of a head movement that took the head away from the center position, and passed the T_m and T_t thresholds. To do this, we took the portion of the head movement where the absolute value of the start angle of the movement was smaller than the absolute value of the end angle. This was truncated so that only the portion that was on one side of the zero line was taken. We then subjected this remaining movement to time and magnitude thresholds (see above). If it passed, it was counted as a scan (Figure A1).

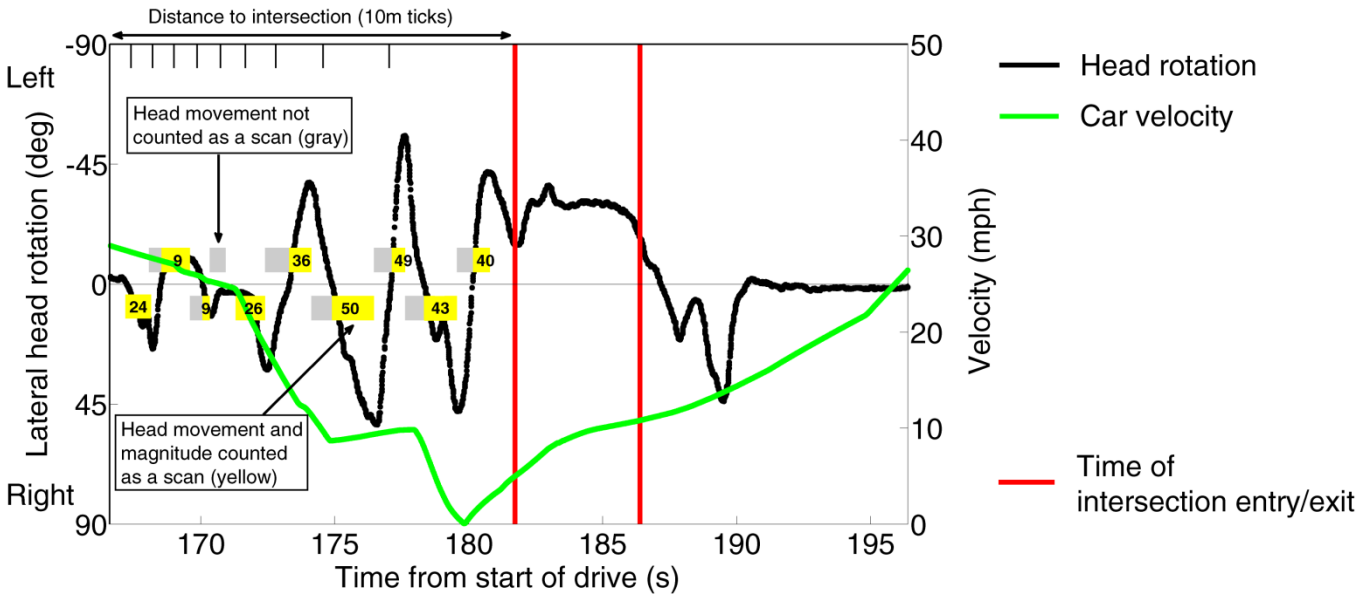

Figure A1 Plot of lateral head rotation (black line) for a participant with RHH on approach to a T-intersection with a stop sign and incoming roads on both sides. As the participant's car approached the intersection, the head rotations increased in magnitude and car velocity (green line) decreased to zero. After stopping, the participant executed a left turn. Nine head scans, rotations that took the head away from the center position, were identified by the algorithm (yellow bars; 4 scans to the left and 5 to the right). Only those rotations that exceeded a specific time and angular magnitude threshold were counted as scans. Gray bars represent head rotation that was not a scan. Yellow bar represents the portion of the head movement that was counted as a scan (magnitude in degrees is indicated). Upper axis contains tick marks at every 10 m from the intersection.

REFERENCES

1. Mandel AJ, Bowers AR, Goldstein RB, Peli E. Analysis of driving behavior where it matters. In: *Proceedings of the Driving Simulator Conference (DSC) North America 2007*. Iowa City, IA, 2007: DVD-ROM. 181-190.
2. Reed MP, Green PA. Comparison of driving performance on-road and in a low-cost simulator using a concurrent telephone-dialling task *Ergonomics.* 1999;42:1015-1037.
3. Oppenheim A, Schafer R. *Discrete-time signal processing.* Upper Saddle River, NJ: Prentice Hall; 1989.

APPENDIX 2: Head Movement Plots For Intersections With Pedestrians

At intersections with I-Peds, head scans in the direction of the I-Ped were analyzed between the time when the I-Ped appeared, and either the time of the horn press or the time when the I-Ped disappeared, whichever occurred first (see Figures A2.1 to A2.4 below). Each I-Ped event was then categorized as: (1) driver failed to scan in the direction of the I-Ped and did not detect; (2) driver scanned in the direction of the I-Ped but did not detect; or (3) scanned in the direction of the I-Ped and detected.

I-Ped A at the extreme left of the intersection

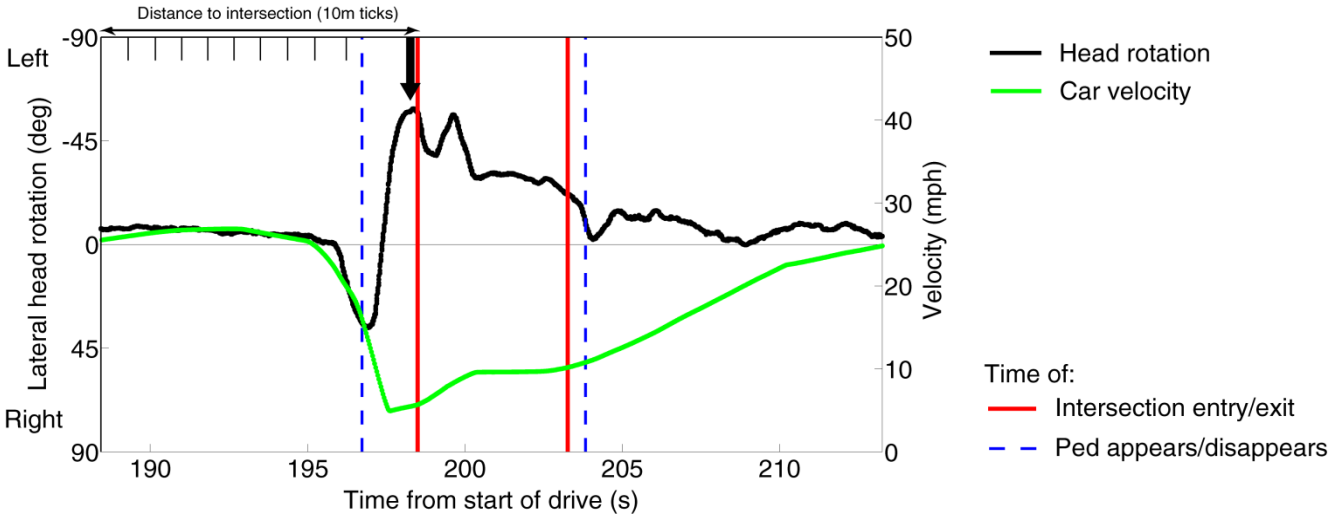

Figure A2.1 Participant with RHH detected I-Ped A on a left turn at a T-intersection with incoming roads on both sides. The pedestrian appeared during a rightward scan (at about 197 s). At the end of the subsequent leftward scan, the horn was pressed (large black arrow) to indicate detection. The left scan magnitude (about 56°) was sufficient for the I-Ped to be seen on the seeing side. Note that the first head scan was to the blind right side.

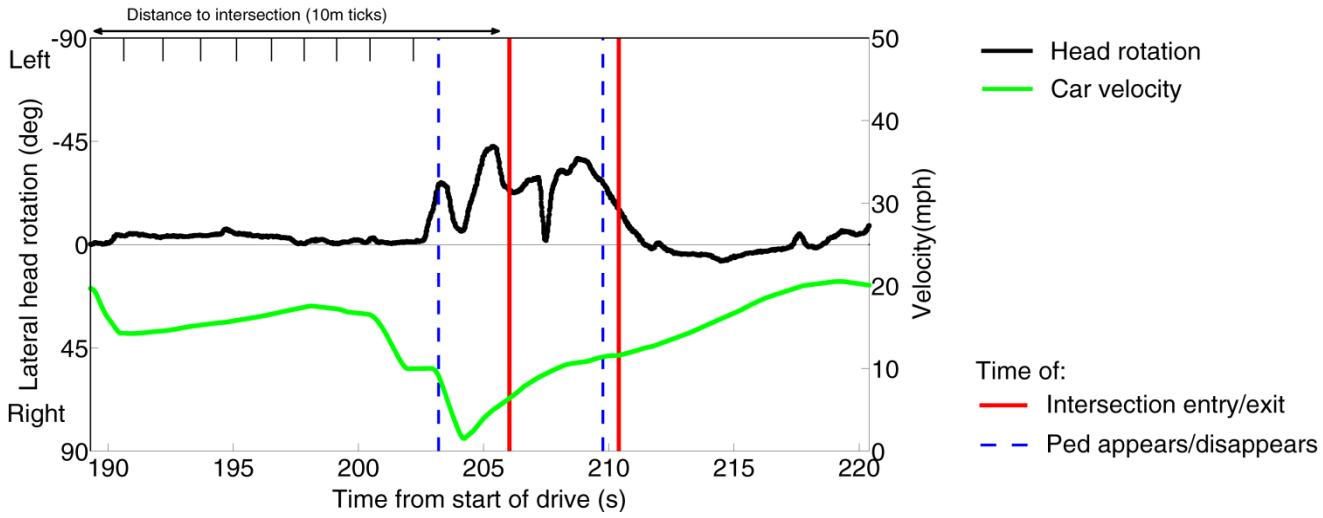

Figure A2.2 Participant with LHH failed to detect I-Ped A on a left turn at a T-intersection with incoming roads on both sides. The pedestrian appeared during the first leftward head scan (at about 204 s), which was followed by another leftward scan before entering the intersection. However, the magnitude of the second leftward scan (about 37°) was insufficient for the I-Ped to be seen on the blind side. Note that the first head scan was to the blind left side and there were no scans to the seeing right side before entering the intersection.

I-Ped D at the extreme right of the intersection

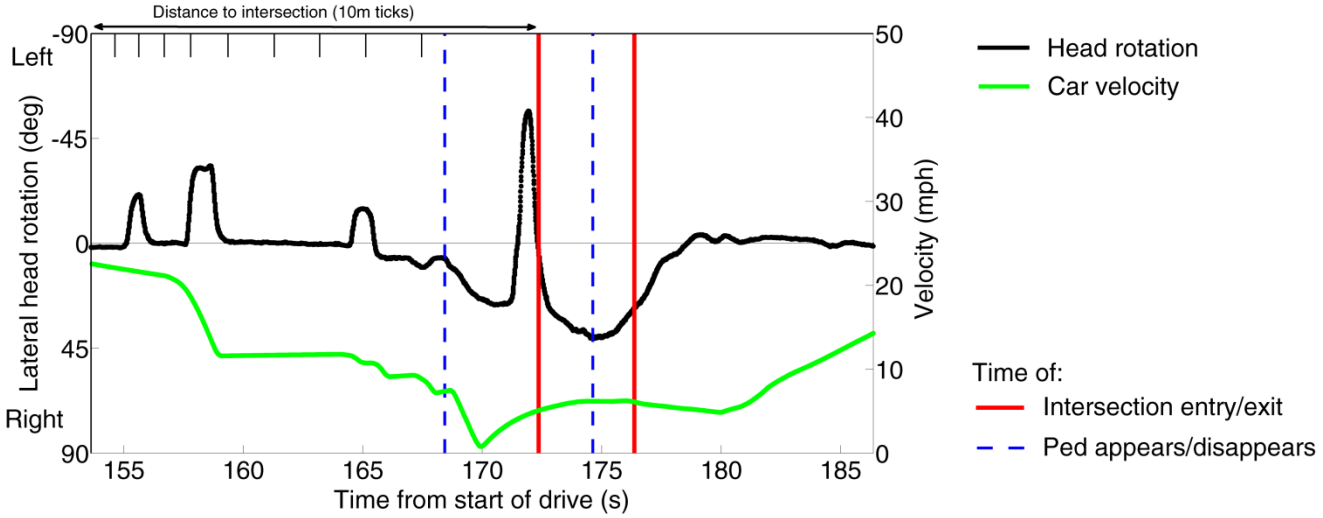

Figure A2.3 Participant with RHH failed to detect I-Ped D on a right turn at a T-intersection with incoming roads on both sides. After the pedestrian appeared (at about 168 s), there was a large leftward scan (about 52°); however, there was no rightward scan before entering the intersection.

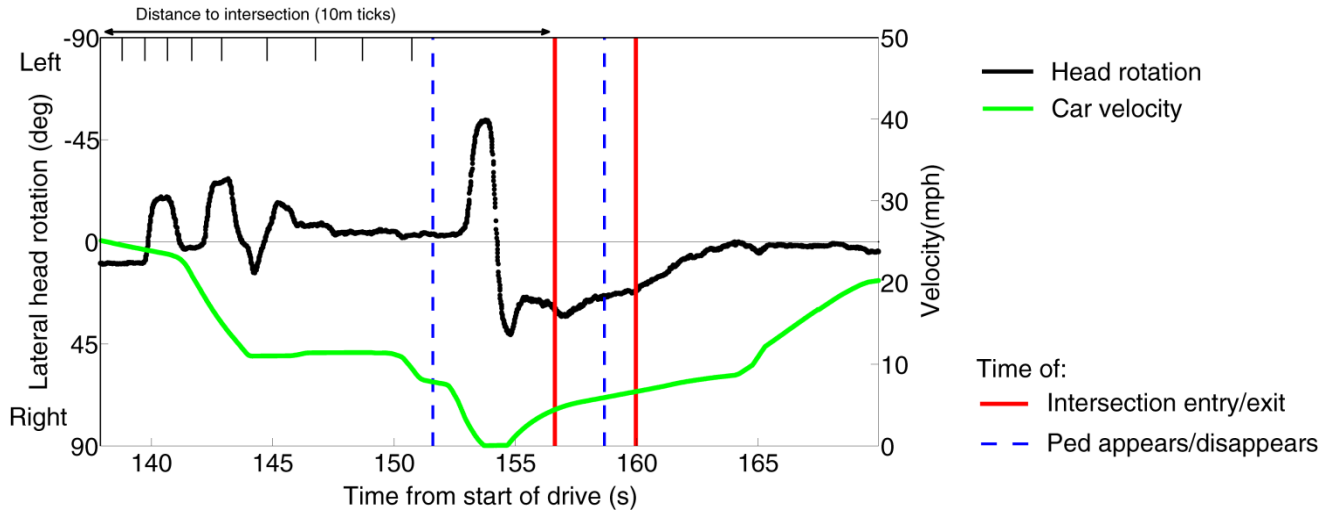

Figure A2.4 Participant with RHH failed to detect I-Ped D on a right turn at a T-intersection with incoming roads on both sides. After the pedestrian appeared (at about 151 s), there was a leftward scan followed by a rightward scan, but the magnitude of the rightward scan (about 38°) was insufficient for the I-Ped to be seen on the blind side. By comparison, the leftward scan was about 50°.